Transactions of the Korean Nuclear Society Spring Meeting
Jeju, Korea, May 7-8, 2015

Development of an electrical sensor for measurement of void fraction and identification of flow regime in a horizontal pipe

Woo Yeon Won[a], Min Seok Ko[b], Bo An Lee[c], Yeon Gun Lee[a], Sin Kim[d*]
[a]*Department of Nuclear and Energy Engineering, Jeju National University, Jeju 690-756, Korea*
[b]*Nuclear Safety Research Center, Chung-Ang University, Seoul 156-756, Korea*
[c]*Institute for Nuclear Science and Technology, Jeju National University, Jeju 690-756, Korea*
[d]*School of Energy Systems Engineering, Chung-Ang University, Seoul 156-756, Korea*
**Corresponding author: sinkim@cau.ac.kr*

1. Introduction

The void fraction in two-phase flows is one of the most important parameters in system analysis and design. For this reason, many techniques to measure the void fraction have been proposed. Among them, the electrical impedance technique has a variety of advantages such as easy implementation, no intrusiveness into the flow field, no radiation, and convenient mobility. Due to these merits, the electrical impedance technique has drawn much attention and various designs of the electrical impedance sensor have been proposed. The proposed types of electrical sensors include plate-type [1-5], ring-type [3, 6-9], helical-type [10, 11], internal [12], and wire electrodes [13].

The electrical signals of the electrical impedance sensor depend on the flow structure as well as the void fraction. For this reason, the electrical responses to a given void fraction differ according to the flow pattern. For reliable void fraction measurement, hence, information on the flow pattern should be given.

Based on this idea, a new improved conductance sensor is proposed in this study to measure the void fraction and simultaneously determine the flow pattern of the air-water two-phase mixture in a horizontal pipe. The proposed sensor is composed of a 3-electrode set of adjacent and opposite electrodes. The opposite electrodes measures the void fraction, the adjacent electrode serves to determine the flow patterns.

Prior to the real applications of the proposed approach, several numerical calculations based on the FEM are performed to optimize the electrode and insulator sizes in terms of the sensor linearity. The numerical results are assessed in comparison with the data from static experiments. The sensor system is applied for a horizontal flow loop with 40 mm in inner diameter and 5 m in length and its measurement performance for the void fraction is compared with that of a wire-mesh sensor system.

2. Numerical analysis for sensor optimization

2.1. Mathematical background

Let us consider staratified flow and annular flow through the conductance sensor as shown in Fig. 1.

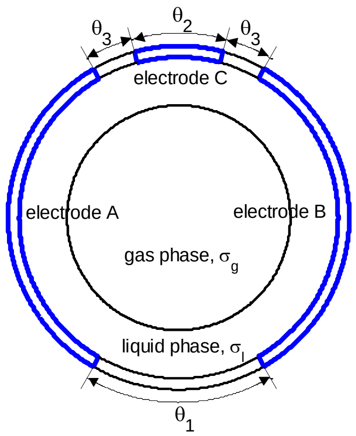

(a) Annular flow

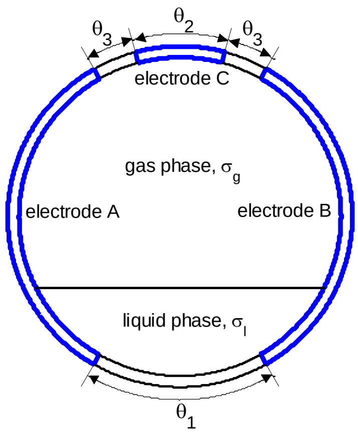

(b) Stratified flow

Fig. 1. Stratified and annular flow through the conductance sensor

In each phase, the potential distribution can be described by the following Laplace equations:

$$\nabla \cdot \sigma_g \nabla u_g = 0 \text{ for the gas phase,} \quad (1a)$$

$$\nabla \cdot \sigma_\ell \nabla u_\ell = 0 \text{ for the liquid phase,} \quad (1b)$$

where u_g and u_ℓ represent the potential distribution to be determined for each phase.

For convenience, we define the dimensionless conductance as:

$$G^*_{opp} = \frac{G}{G_\ell}. \quad (2)$$

Here, G_ℓ is the conductance value in the opposite electrodes for the sensor measured when the flow channel is filled only with liquid ($\alpha = 0$) and G is the measured conductance of two-phase flow.

2.2. Numerical calculations and results.

For 3D numerical calculations, COMSOL Multiphysics based on the FEM was employed. The insulation conditions were used for all boundaries except activated electrodes. Each electrode and insulator angle ranging from 0.1 to 0.5 rad by 0.1 rad was considered. Also, the full range of the void fractions ($\alpha = 0 \sim 1.0$) was taken into account for stratified flow and the void fraction ranging from 0.5 to 1.0 by 0.05 ($\alpha = 0.5 \sim 1.0$) were tested in the case of annular flow because the void fraction is generally above 0.76 in annular flow of horizontal pipes [14].

To find the optimal electrode and insulator sizes, the following nonlinearity error was introduced:

$$\text{Nonlinearity error} = \left| G^*_{linear} - G^*_{opp} \right|_{\max} \times 100 \ (\%), \quad (3)$$

Where G^*_{linear} is the linear conductance response ($G^*_{linear} = \alpha$) and G^*_{opp} is the calculated dimensionless conductance for given void fractions and geometrical parameters (see Eq. (2)).

Figure 2 shows the numerical trends of the nonlinearity error for θ_1. It can be seen from the results that the sensor with larger size of the insulator has better linearity. Summarizing the whole numerical result it is proposed that the sensor linearity is optimized when θ_1, θ_2, and θ_3 are 0.5, 0.2, and 0.3 rad, respectively. With this geometric arrangement the nonlinearity errors for annular flow and stratified flow are 5.7% and 12.7%, respectively.

2.3. Sensor system setup and verification of numerical results

A conductance sensor was fabricated following the dimensions determined in the numerical calculations. The inner diameter of the sensor is 40 mm and three electrodes with 2 mm in thickness are flush mounted on the inner wall of the pipe. The insulator angle in the bottom are $\theta_1 = 0.5$ rad and those for the insulator in the top and the electrode C are $\theta_2 = 0.2$ rad and $\theta_3 = 0.3$ rad, respectively.

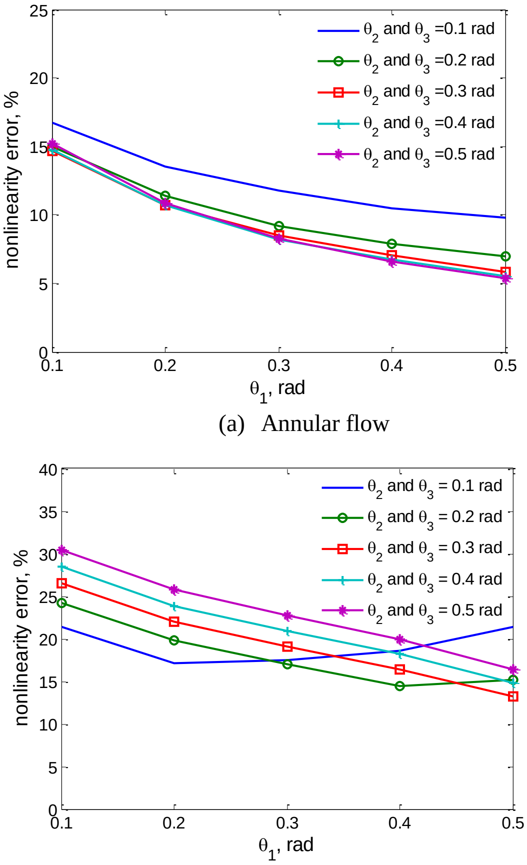

(a) Annular flow

(b) Stratified flow

Fig. 2. The nonlinearity error for θ_1

For measurement, an LCR meter was adopted for voltage sources to the electrodes and switch matrix module and data acquisition devices was employed to shift the voltage sources and data acquisition. The specifications of the measurement instruments used in the experiments are summarized in Table I.

In the experiments the applied voltage was set to 5 V with 10 kHz signal frequency. In this frequency range the electrical response is nearly conductive [6, 7, 17, 18, 19].

Table I. Specifications of measurement instruments used for experiments

Instruments	Accuracy	Signal range	Time definition
Agilent 4284A LCR meter	0.05 ~ 0.5%*	Up to 20 V with 1 MHz	N/A
NI PXI-2536	N/A	Up to ±12 V and 100 mA	50,000 cross-points/sec
NI PXIe-6368	3 mV for ±10V range	Up to ±10 V	2,000,000 samples/channel

* The accuracy is determined depending on the magnitude of the applied voltage. For 1 ~ 10 V range, for example, the basic accuracy is given by 0.1%.

The switch and sampling frequencies of the conductance sensor system were set to 1 kHz and 10 kHz, respectively. With this setup, 10 electrical conductance values are first measured in the adjacent electrode pair and those are consecutively recorded in the opposite pair. This measurement procedure is repeated at a rate of 1 kHz.

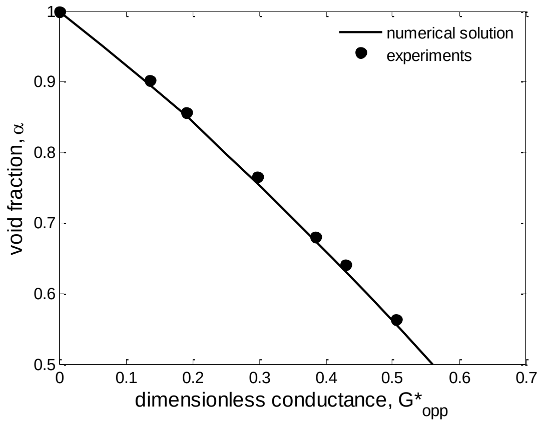

Fig. 3. Comparison between numerical solutions and static experimental results for annular flow

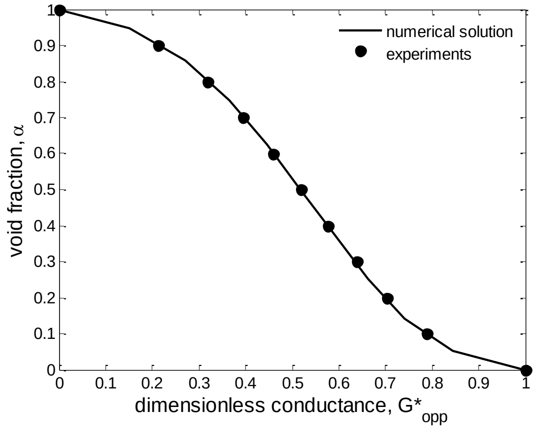

Fig. 4. Comparison between numerical solutions and static experimental results for stratified flow

Figures 3 and 4 show the comparison results between the numerical solutions and preliminary static experimental data for annular flow and stratified flow, respectively. For both cases, the experimental results show very good agreements with the numerical predictions. The nonlinearity errors for annular flow and stratified flow are about 7.0% and 12.0%, which are comparable to those of the numerical calculations (5.7% for annular flow and 12.7% for stratified flow).

3. Experimental results and discussions

In order to verify the electrical sensor from the actual two-phase flow, the dynamic experiments was performed by using a horizontal loop. For the loop experiments various superficial velocities ranging from 0.05 to 1.2 m/s for water ($j_\ell = 0.05 \sim 1.2$ m/s) and from 0.8 to 14.7 m/s for air ($j_g = 0.8 \sim 14.7$ m/s) were considered. Some selected flow conditions discussed here are given in Table II and illustrated on the experimental flow pattern map of Mandhane et al [15] as shown in Fig. 5.

In the experiments, the switch and sampling frequencies of the conductance sensor were set identical to those for the static experiments and the measurement frame of the wire-mesh sensor was set to 10 kHz. These two sensor systems were synchronized by a customized clock box.

Table II. Specifications of measurement instruments used for experiments

Case	j_ℓ (m/s)	j_g (m/s)	Flow pattern
01	0.05	7.9	Stratified flow
02	0.1	7.7	Stratified flow
03	0.4	7.1	Intermittent flow
04	0.56	6.6	Intermittent flow
05	0.76	6.5	Intermittent flow
06	0.9	6.8	Intermittent flow
07	0.2	4.2	Intermittent flow
08		6.3	Intermittent flow
09		8.5	Intermittent flow
10		10.8	Intermittent flow
11		12.7	Intermittent flow
12		14.2	Intermittent flow

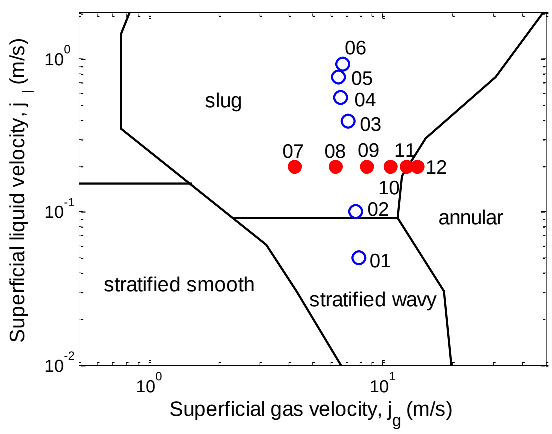

Fig. 5. Some selected flow cases on the flow regime map of Mandhane et al. (1974)

Criteria for the flow pattern in the horizontal pipe were determined based on the existing research [14, 16]. In the present work three flow patterns (stratified flow, annular flow and intermittent flow) are considered. The criteria for flow pattern classification in this study are summarized as follows:

$$G^*_{adj} < 0.005 \text{ for stratified flow,} \tag{4a}$$

$$G^*_{adj} \geq 0.005 \text{ and } G^*_{opp} < 0.3 \text{ for annular flow,} \tag{4b}$$

$$G^*_{adj} \geq 0.005 \text{ and } G^*_{opp} \geq 0.3 \text{ for intermittent flow.} \tag{4c}$$

For the identified flow pattern, the conductance response measured in the opposite electrodes is directly converted into the void fraction through the calibration curves shown in Figs. 3 and 4. For intermittent flow, both numerical and experimental simulations are not straightforward due to complexity of the interface. This work assumes that the intermittent flows belong to the stratified flows, rather than the annular flows.

Figure 6 shows the comparison result between the conductance sensor (CS) and the wire-mesh sensor (WMS). The number '1', '2', and '3' on the y axis of the bottom figures represent the flow pattern criteria (4a), (4b), and (4c), respectively.

The measurement results of the proposed sensor are generally in good agreements with those of the wire-mesh. Figure 7 shows the comparison results for the time-averaged void fraction. Very good agreements between the proposed sensor and the wire-mesh sensor are observed. For all flow rate conditions, the maximum deviation between two instruments is 6.3%. However, the void fractions in the proposed sensor show relatively underestimated values compared to data from the wire-mesh sensor.

In the practical two-phase flows, the bubbles might be contained in the liquid phase or the liquid droplets might be suspended in the gas phase. The wire-mesh sensor can somewhat account for these local phenomena while the conductance sensor essentially has difficulties in detecting them due to its own mechanical structure and measurement modality. These different features of the wire-mesh sensor and the conductance sensor might cause some deviations. Also, in the present work the concentric annular flow was considered. This might be a good approximation for stable annular flows. However, this could give rise to some errors in the case that the liquid film distribution is significantly asymmetric and the unstable film is formed on the electrode walls. Although the measurement speed of the proposed sensor is overall fine compared to the wire-mesh sensor, its limitations observed in the experiments have to be further improved in future works.

4. Conclusion

In this study, an electrical sensor for measuring the void fraction and identifying flow pattern in horizontal pipes has been designed. For optimization of the sensor, numerical analysis have been performed in order to determine the geometry and verified it through static experiments. Also, the loop experiments were conducted for several flow rate conditions covering stratified and intermittent flow regimes and the experimental results for the void fractions measured by the proposed sensor were compared with those of a wire-mesh sensor. The comparison results are in overall good agreements. However, due to the difficulties in detecting the local phenomena in the proposed sensor, it generally showed underestimated values compared to data from the wire-mesh sensor. Nevertheless, the maximum deviation within 6.5% showed the feasibility of the proposed conductance sensor.

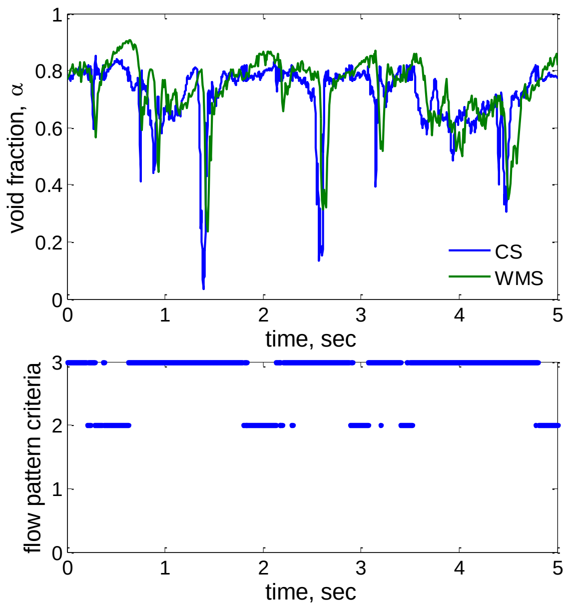

Fig. 6. Comparison in instantaneous void fraction between CS and WMS for superficial liquid velocities (case 5).

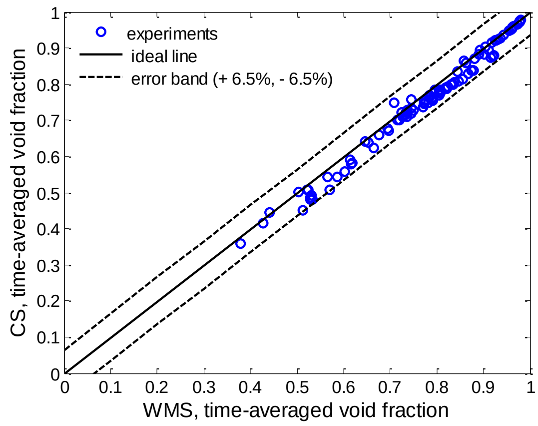

Fig. 7. Comparison in time-averaged void fraction between CS and WMS

Acknowledgement

This research was supported by Basic Science Research Program through the National Research Foundation of Korea (NRF) funded by the Ministry of Education. (No. NRF-2010-0020077)

REFERENCES

[1] Kendoush A A and Sarkis Z A, Void fraction measurement by x-ray absorption Exp. Therm. Fluid Sci. Vol. 25, pp. 615-621, 2002.

[2] Lowe D C and Rezkallah K S, Flow regime identification in microgravity two-phase flows using void fraction signals Int. J. Multiph. Flow Vol.17, pp.433-457, 1999

[3] Ahmed W H, Capacitance sensors for void-fraction measurements and flow-pattern identification in air-oil two-phase flow, IEEE Sensors J. Vol. 6, pp. 1153-1163, 2006.

[4] Canière H, T'Joen C, Willockx A and De Paepe M, Capacitance signal analysis of horizontal two-phase flow in a small diameter tube Exp. Therm. Fluid Sci. Vol. 32, pp.892-904, 2008

[5]Kim S, Lee J S, Kim K Y, Kang K H and Yun B J, An approximate formula for the capacitance-void fraction relationship for annular flows Meas. Sci. Technol. Vol.20, pp.125404, 2009b

[6] Andreussi P, Di Donfrancesco A and Messia M, An impedance method for the measurement of liquid hold-up in two-phase flow, Int. J. Multiph. Flow Vol. 14, pp. 777-785, 1988.

[7] Tsochatzidis N A, Karapantsios D K, Kostoglou M V and Karabelas A J A conductance probe for measuring liquid fraction in pipes and packed beds Int. J. Multiph. Flow Vol.18, pp.653-667, 1992.

[8] Kim J R, Ahn Y C and Kim M H, Measurement of void fraction and bubble speed of slug flow with three-ring conductance probes Flow Meas. Instrum. Vol.20, pp.103-109, 2009a.

[9] Rosa E S, Flora B F and Souza M A S F, Design and performance prediction of an impedance void meter applied to the petroleum industry Meas. Sci. Technol. Vol.23, pp.055304, 2012.

[10] Geraets J J M and Borst J C, A capacitance sensor for two-phase void fraction measurement and flow pattern identification Int. J. Multiph. Flow Vol. 14, pp. 305-320, 1988.

[11] Ye J, Peng L, Wang W and Zhou W, Optimization of helical capacitance sensor for void fraction measurement of gas-liquid two-phase flow in a small diameter tube IEEE Sensors J. Vol.11, pp.2189-2196, 2011.

[12] Yang H C, Kim D K and Kim M H Void fraction measurement using impedance method Flow Meas. Instrum. Vol.14, pp.151-160, 2003.

[13] Huang S, Zhang X, Wang D and Lin Z, Equivalent water layer height (EWLH) measurement by a single-wire capacitance probe in gas-liquid flows Int. J. Multiph. Flow Vol. 34, pp. 809-818, 2008.

[14] Barnea D, Transition from annular flow and dispersed bubble flow – unified models for the whole range of pipe inclinations Int. J. Multiph. Flow Vol. 12, pp. 733-744, 1986.

[15] Mandhane J M, Gregory G A and Aziz K A flow pattern map for gas–liquid flow in horizontal pipes *Int. J.* Multiph. Flow Vol.1, pp.537–553, 1974.

[16] Taitel Y and Dukler A E, A model for predicting flow regime transitions in horizontal and near horizontal gas-liquid flow AICHE J. Vol.22, pp.47-55, 1976.

[17] Fossa M, Design and performance of a conductance probe for measuring the liquid fraction in two-phase gas-liquid flows Flow Meas. Instrum. Vol. 9, pp. 103-109, 1998

[18] Song C H, Chung M K and No H C. Measurements of void fraction by an improved multi-channel conductance void meter Nucl. Eng. Des. Vol.184, pp.269-285, 1998.

[19] Devia F and Fossa M, Design and optimisation of impedance probes for void fraction measurements Flow Meas. Instrum. Vol. 14, pp. 139-149, 2003.